doi: 10.5028/jatm.v10.958 ORIGINAL PAPER

Research on the Folding Patterns and Deployment Dynamics of Inflatable Capsule Structures

Yi-hong Hong[1,2], Wen-juan Yao[1], Yan Xu[3], Tingchen Fang[4]

Hong Y http://orcid.org/0000-0003-4178-2400
Yao W http://orcid.org/0000-0002-1890-3035
Xu Y http://orcid.org/0000-0003-4718-1681
Fang T http://orcid.org/0000-0002-9609-8633

How to cite

Hong Y; Yao W; Xu Y; Fang T (2018) Research on the Folding Patterns and Deployment Dynamics of Inflatable Capsule Structures. J Aerosp Technol Manag, 10: e4718. doi: 10.5028/jatm.v10.958.

ABSTRACT: The folding patterns and deployment dynamic characteristics of conical inflatable capsule structures were investigated. A six-fold-line method of packing a conical shell surface was designed. The fold-line layouts and relation formulas of the fold angles were determined. The folded state of the inflatable capsule structure was parametrically modeled; then, the deployment dynamic analysis model was established using ANSYS/LS-DYNA software. The dynamic characteristics of the inflatable capsule structure in orbit were numerically simulated. Thus, the deployment configurations and the time history curves of the dynamic characteristics were obtained. The results verified the feasibility of the fold pattern and the deployment dynamic analysis model. The influences of the residual gases from the packing process on the subsequent deployment process were investigated. The results indicated that a small amount of residual gas can lead to structures that cannot deploy smoothly, and two methods were presented to avoid this challenge. These works provide technical support for the structural designs of this type of inflatable capsule structure.

KEYWORDS: Inflatable capsule structures, Folding pattern, Deployment dynamics, Residual gas.

INTRODUCTION

For large, lightweight aerospace structures, inflatable structure technology is ideal. With the advantages of a lower manufacturing cost, lighter weight, and smaller launch volume, inflatable capsule structures have been widely used in spacecrafts (Xu *et al.* 2012), weapon equipment and building structures. In recent years, a novel inflatable reentry vehicle was proposed for the Mars exploration project. A conical inflatable capsule structure would be formed before reentry and provide the aerodynamic drag force. In 2012, IRVE-3 was successfully launched by NASA (Lichodziejewski *et al.* 2012). In manned spaceflight, an inflatable capsule structure can be used to build inflatable modules and lunar habitats (Xu *et al.* 2016). The Bigelow Expandable Activity Module (BEAM) is an experimental inflatable capsule structure used as a test temporary module on the International Space Station (ISS) and has been successfully expanded and pressurized after the first attempt failed in 2016.

1.Shanghai University – Department of Civil Engineering – Shanghai – China. **2.**Quzhou University – School of Architectural Engineering – Zhejiang – China. **3.**Zhejiang University – School of Aeronautics and Astronautics – Zhejiang – China. **4.**Shanghai Construction Group Co. LTD –Shanghai – China.

Correspondence author: Wen-juan Yao | Shanghai University – School of Architectural Engineering – Department of Civil Engineering | Shangda road 99 | CEP: 200072 – Shanghai – China | E-mail: wjyao2016@163.com

Received: Jul. 4, 2017 | **Accepted:** Dec. 15, 2017

Section Editor: Dimitrius Pavlou

One of the key technologies in inflatable capsule structures is that the system can be folded and expanded. Following the experiences with the BEAM inflatable capsule structures, detailed numerical investigations of the folding pattern and deployment mechanisms of these structures are necessary. To date, research of the deployment mechanism has primarily focused on inflatable tubes. A deployment simulation model was proposed by Haug *et al.* (1991) that used the explicit nonlinear finite element software PAM – CRASH to simulate an inflatable support ring and reflector. The dynamic simulation of a space inflatable tube was finished by Wang and Johnson (2003). An inflatable tube between two-fold points is equivalent to a cantilevered beam and was simulated based on a nonlinear hinge model by Clem *et al.* (2000). The dynamical analysis method of the inflatable tube was developed based on the contact mechanics and fluid mechanics of the deployment of inflatable tubes with one fold point, as observed in experiments (Bouzidi *et al.* 2013). However, these works were focused on individual inflatable components and the effects of residual stress and residual gas in the inner chamber were ignored, although they require further investigation. The deployment mechanisms of inflatable tubes under restricted conditions were analyzed using ABAQUS/Explicit software, and a corresponding experiment was conducted (Sosa *et al.* 2016). A cylindrical inflatable lunar habitat was designed and tested in ILC, and a deployment experiment was conducted on the ground (Hinkle *et al.* 2009). Also, the deployment of an inflatable tube was validated by a space experiment (Wei *et al.* 2015). Folding pattern, parametric model methods and a software simulation of the deployment mechanisms of inflatable antenna structures were then investigated in detail (Xu *et al.* 2015).

Research on folding pattern theories was also focused on inflatable tubes. Z-folding patterns of inflatable tubes were studied on the air floating sustainment by Welch *et al.* (2003). Several typical folding pattern theories for inflatable tubes were studied, such as the quadrilateral folding pattern, octagon folding pattern, and hexagon folding pattern. The characteristics of the various theories were noted by Schenk *et al.* (2014). However, a certain degree of residual stress exists in the membrane material for the existing fold pattern theories, and the common Z-fold pattern and wrapping fold pattern suffer from poor ventability of residual gases, which may cause an unstable deployment process.

Despite the abovementioned research and development efforts, the folding patterns and deployment dynamics of the inflatable capsule structures with surface shapes other than tubes still need to be investigated. The inner chamber of the inflatable capsule structures is difficult to pump to an absolute vacuum during the packing process. Due to the leakage of membrane materials, residual gases in the capsule body are inevitable. The effects of residual gases during the packing and the expansion process must be studied. This paper reports a recently conducted effort that systematically addressed some of these issues for a conical inflatable capsule structure. The six-fold-line folding pattern and deployment dynamic analysis model of an inflatable capsule structure were investigated, and the influence of residual gases was considered in the deployment dynamic analysis model.

The remainder of this paper consists of four sections. The next section presents the formulation of a six-fold-line method of folding conical inflatable capsule structures, and the fold-line layouts are determined. The fold state of the inflatable capsule structure was parametrically modeled. Then, the deployment dynamic analysis model using ANSYS/LS-DYNA software is described. The dynamic characteristics of the inflatable capsule structures in orbit were numerically simulated. The influences of residual gases on the subsequent deployment process are investigated next, as are two methods meant to void this challenge. Finally, the last section summarizes a few concluding remarks and suggestions for future work.

FOLDING PATTERN OF CONICAL INFLATABLE CAPSULE STRUCTURES

NECESSARY CONDITIONS FOR THE SURFACE FOLDING

Given the necessary conditions of the plane membrane folding pattern, a six-fold-line method for packing curved surfaces (meshed into several plane) was proposed. With six fold lines, the tangent plane of the curved surface is divided into six portions. As shown in Fig. 1, four lines are mountain lines (shown as the solid lines OA, OB, OC and OD in Fig. 1) and two lines are valley lines (shown as the dotted lines OE, and OF in Fig.1). The angle between the two valley lines at the folded point is δ. The necessary condition for full folding is (Eq. 1)

$$\beta_1 - \alpha_1 = \beta_2 - \alpha_2 + \delta \tag{1}$$

where these angles are the angles between the space fold lines:

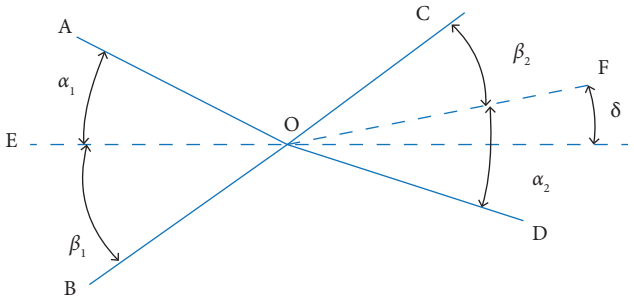

Figure 1. Six-fold-line method.

FOLDING PATTERN DESIGN OF A CONICAL SURFACE

Mesh of a conical surface

For the conical surface shown in Fig. 2, the radii of the top and bottom sections are r_1, r_2, the height is H, and half the top angle is φ.

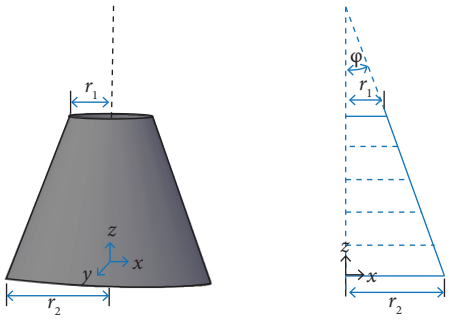

Figure 2. Conical shell surface.

The conical shell surface is divided into M subcones along the longitude direction, and M = 5, as shown in Fig. 2. For the No. 1 subcone surface of conical shell surface in Fig. 2, as shown in in Fig. 3a, the radii of the top section and bottom section are r_{i-1}, r_i, and the subcone can be expanded into a sector plane, as shown in Fig. 3b.

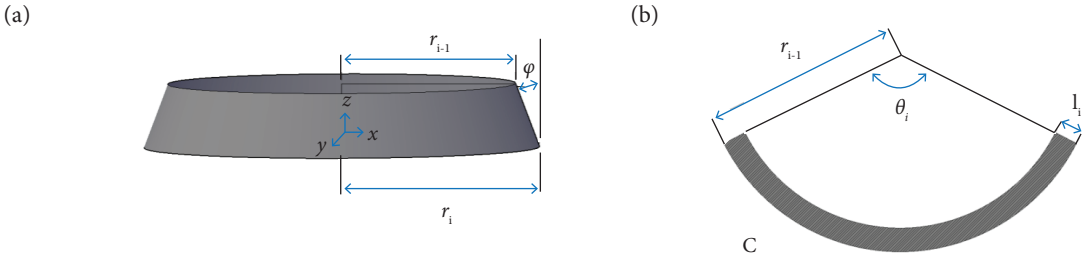

Figure 3. Sub-conical shell surface is expanded. (a) No.1 subcone surface; (b) expanded sector plane.

The center angle and the radius of the outer arc of the corresponding sector region are written as (Eq. 2):

$$\theta_i = 2\pi \sin\varphi$$
$$R_i = r_i / \sin\varphi \tag{2}$$

where: θ_i is center angle of the outer arc, R_i is the radius of the outer arc, r_i is the radii of bottom section, φ is half the top angle.

SIX-FOLD-LINE PATTERN

The central angle of the flattening conical surface is θ_i. The outer arc is divided into N segments along the circumferential direction. Therefore, the whole conical surface is divided into $N \times M$ parallelograms. The six-fold-line pattern of the expanded sector plane in Fig. 3b is shown in Fig. 4a, and there are 6 parallelograms. One of the parallelograms is shown in Fig. 4b. There are N parallelograms in one subcone that are symmetric distributed around the center node O. The corresponding central angle of line AD is expressed as θ_2, and ϕ denotes the angle ∠KAD.

Triangle OAB, OKD, the ODE are isosceles triangles, so (Eq. 3)

$$\angle OAB = \angle OBA = \frac{\pi}{2} - \frac{\theta_1}{2} \tag{3}$$

where: θ_1 is the corresponding central angle of line AB and line DE in the first quadrilateral. There is $\theta_1 = \theta/N$.

The inner angles and the angles of the four sides and the line AE are defined as α_1, β_1, γ_1, α_2, β_2, γ_2, which must be consistent for each parallelogram (Eq. 4):

$$\gamma_1 = \angle OBA + \varphi = \frac{\pi}{2} - \frac{\theta_1}{2} + \phi \tag{4}$$

In the triangle ABE, there is (Eq. 5)

$$\beta_2 = \frac{\pi}{2} + \frac{\theta_1}{2} - \alpha_1 - \phi \tag{5}$$

Then (Eq. 6)

$$\beta_1 = \frac{\pi}{2} - \frac{\theta_1}{2} - \alpha_1 - \phi \tag{6}$$

In the triangle AKD, there are ∠AKD = (л/2) + (θ_2/2) and ∠AKD = (л/2) + (θ_2/2) – ϕ. From all the angles around point D, we have (Eqs. 7-8)

$$\gamma_2 = 2\pi - (\angle ODK + \angle ODE + \angle ADK) = \frac{\pi}{2} + \theta_2 + \phi + \frac{\theta_1}{2} \tag{7}$$

$$\alpha_2 = \alpha_1 - \theta_2 \tag{8}$$

where: α_1, α_2 are the angles between the space fold lines, as shown in Fig. 4.

While the geometric sizes of the conical surfaces and the number N of the outer arcs are determined, the length of side AB and the corresponding central angle θ_1 can be calculated. All the angles and lengths of each parallelogram can be obtained after α_1, ϕ are known.

Whether the six-fold-line pattern meets the necessary condition of Eq. 1 is proved as follows:

There are three parallelograms around the fold point E is shown in Fig. 5. As shown in Fig. 5, the angles are related as follows: ∠ODE = ∠OAB = $\phi + \alpha_1 + \beta_1$, ∠ADI = $\phi + \theta_2$ and ∠ADE = ∠IDE + ∠ADI = л – ∠ODE + ∠ADI = л – ($\alpha_1 + \beta_1$) +θ_2, and ∠ADE = л – ($\alpha_2 + \beta_2$) in the triangle ADE. Therefore, it follows from these equations that (Eq. 9)

$$\alpha_2 = \alpha_1 - \theta_2 \tag{9}$$

and in the triangle OBA, ∠OBA = π – $(\alpha_1 + \beta_1)$ +θ_1 – ϕ, while ∠OBA = π – $(\alpha_1 + \beta_2)$ + ϕ, in the triangle AEB. Therefore (Eq. 10),

$$\beta_2 - \alpha_2 = \beta_1 - \alpha_1 + \theta_1 + \theta_2 \tag{10}$$

where: β_1, β_2 are the angles between the space fold lines, as shown in Fig. 4.

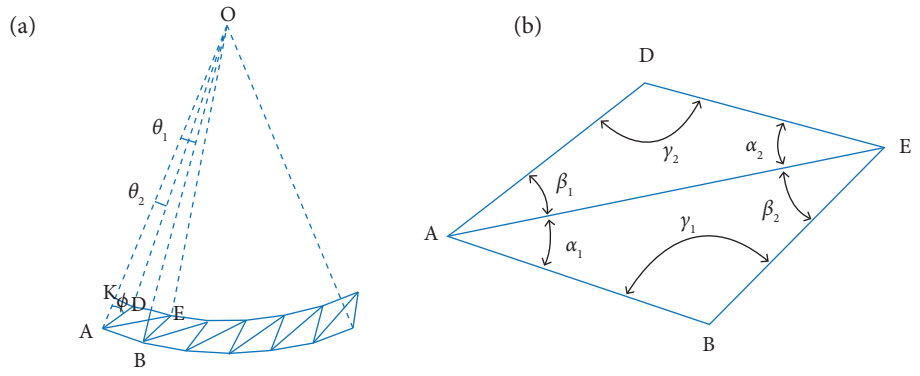

Figure 4. Six-fold-line method. (a) Six-fold-line pattern of expanded sector plane; (b) one of the parallelograms.

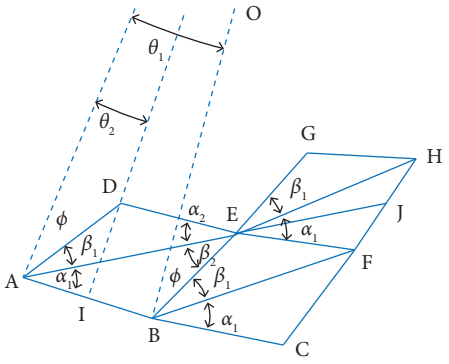

Figure 5. Parallelograms around the fold point E.

In the triangle OAE, ∠AOE = θ_1 + θ_2. Thus, ∠OEJ = θ_1 + θ_2 + β_1 + ϕ can be found. In addition, ∠OEH = β_1 + ϕ, so the angle between the line EJ of the fold line AE and the fold line EH is calculated as follows (Eq. 11):

$$\angle HEJ = \theta_1 + \theta_2 \tag{11}$$

Given the upper two equations (Eqs. 10-11), the six-fold-line pattern at point E satisfies the necessary conditions of Eq. 1.

After the folding pattern of the conical surface is determined, the folded state can be obtained after it is folded through several fold steps. As shown in Fig. 6, using two adjacent parallelograms, ABDE and BCEF, as an example, state (a) is folded along the fold line AE to obtain state (b); the parallelogram BCEF becomes B'C'EF'. Then, it is folded along the fold line B'E to get state (c), turning the parallelogram B'C'EF' into B'C"EF". Finally, triangle B'C"F" is folded along the fold line B'F", and state (d) is reached. Now point C" moves to point C"'.

In state (c), ∠AEB' = ∠AEB' = β_2, ∠F"B'E = ∠EAD = β_1, so the angle between the two fold lines of AE and B 'F' in the final folded state (d) are expressed in the following form:

$$\varphi = \pi - \beta_1 - \beta_2 \tag{12}$$

Substituting Eqs. 5 and 6 into Eq. 12, the following equation can be obtained (Eq. 13):

$$\varphi = 2(\alpha_1 + \phi) \tag{13}$$

After the conical surface is fully folded, the folded state (d) of the number is N / 2, as shown in Fig. 6, will be rejoined together as a closed loop, and the N fold lines form an N sided positive polygon. The inner angle is $\varphi = \pi - (2\pi/N)$, so

$$\alpha_1 + \phi = \frac{\pi}{2} - \frac{\pi}{N} \tag{14}$$

When the angles satisfy the upper equation, the flattening pattern and fold state of the conical surface can be closed.

The radius of the bottom section of the conical surface is 500 mm, the radius of the top section is 365 mm, and the height is 1000 mm. The number of outer arcs N = 6, and the surface is divided into M = 3 along the longitude direction. The folding angles α_1, ϕ are designed such that $\alpha_1 = \phi = \pi/6$, which satisfies Eq. 14. All the angles and lengths of the parallelograms can be determined. The final folding pattern of the conical surface is shown in Fig. 7.

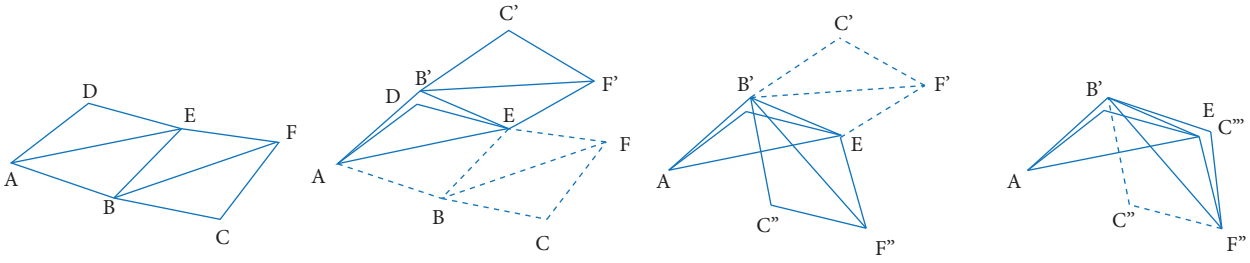

Figure 6. Fold process for a conical surface.

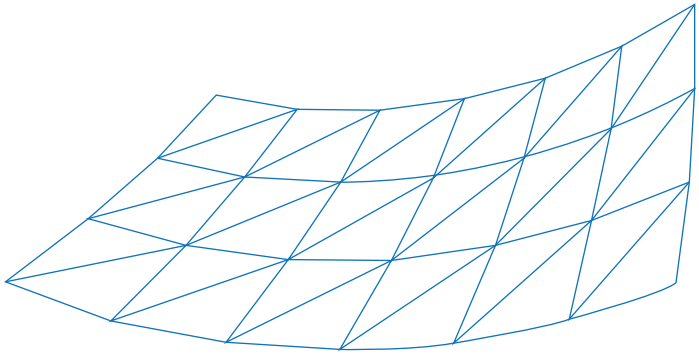

Figure 7. Final folding pattern for conical surface.

In the ANSYS/LS-DYNA software, the numerical fold model of the conical surface is obtained using APDL language, which is shown in Fig. 8. After the folding process, the height of the model is 40 mm; the top and bottom radii are invariant. To better display the fold model, different colors are used for each subcone of the conical surface. When the upper and bottom planar surfaces were assembled, the folded state of the inflatable capsule structures was parametrically modeled.

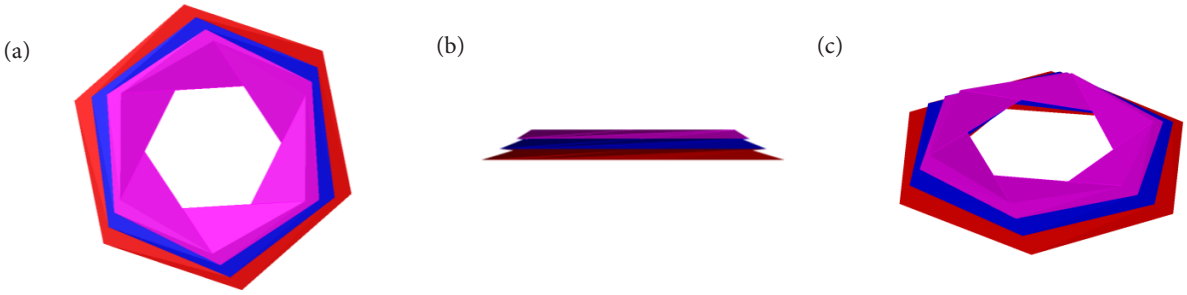

Figure 8. Fold state of the conical shell surface. (a) Planform; (b) Front view; (c) Axonometric.

DYNAMIC MODELING AND SIMULATION OF DEPLOYMENT

DYNAMICS ANALYSIS MODEL OF DEPLOYMENT

The dynamic analysis model of the inflatable capsule structure is built in the finite element software ANSYS/LS-DYNA. The relevant keywords are added in a K file based on the fold state generated in the previous section. The final K file is imported into ANSYS/LS-DYNA; then, the simulation can be conducted. The reliability and stability of the deployment process are important for inflatable structures. If inflated too quickly, the structures will vibrate severely. Thus, inflatable capsule structures are expanded at a low velocity. When the dynamic analysis model is built, the AIRBAG model * AIRBAG_SIMPLE_AIRBAG_MODEL from ANSYS/LS-DYNA is used to simulate the inflatable capsule structures. In this paper, the deployment dynamic analysis is based on the control volume method. The fabric material model is used to simulate the inflatable structures, and the keyword in LS-DYNA is * MAT_FABRIC. Since the material of the inflatable structures cannot be subjected to compressive stress, GSE = 1 is set in the fabric material model.

In the LS-DYNA analysis model, the self-contact problem of inflatable structures must be solved. The contact surface, type of contact, and the contact parameters are defined. The typical contact types consist of single surface contact, node-surface contact and surface-surface contact. When analyzing the inflatable capsule structures, single surface contact is adopted to the dynamics analysis model. The corresponding keyword for this contact type is * CONTACT_AIRBAG_SINGLE_SURFACE, which is used exclusively for self-contact problems of inflatable structures. Contact detection can be automatically performed from the top and bottom sides of the shell element in this contact type, and the contact between the triangle and tetrahedron mesh can be solved with increased stability. The parameter SOFT is set to be 2, which means that the segment-segment contact algorithm is activated. Because the membrane material has a gas penetration after the inflatable structures is folded, the parameter IGNORE is set to be 1. The inflatable gas is nitrogen (N_2), the density of which is 1.221 kg/m^3. The structures are expanded in orbit, and the environmental pressure of the model is 0 Pa. The mass flow rate of the inflatable gas is designed to be 5 g/s.

The radius of the bottom section of the inflatable capsule structures is 500 mm, the radius of the top section is 365 mm, and the height is 1000 mm. The FEA dynamic analysis model of the inflatable capsule structures is shown in Fig. 9. The number of

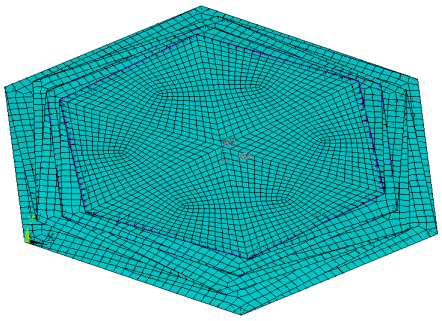

Figure 9. FEA model of the inflatable capsule structures.

shells in the model is 12046, and the number of nodes is 11988. The elastic modulus of the membrane material is 3.45E9 Pa, the Poisson ratio is 0.3, the density is 1.4E3 kg/m^3, and the thickness is 25.4E-3 mm.

DEPLOYMENT DYNAMICS ANALYSIS IN ORBIT

Based on the above dynamic analysis model, an orbital deployment simulation of the inflatable capsule structures was performed with the ANSYS/LS-DYNA software. The deployment configurations during the expansion process were obtained, which is illustrated in Fig. 10. The z-velocity of the center node during the top surface change during the deployment process is shown in Fig. 11. The kinetic energy of the whole system is shown in Fig. 12.

From the curves shown in the figures, the deployment velocities of the free ends have small variations during the inflatable process, and the kinetic energy of the whole structure changes smoothly. The results show that there is no great collision or physical interference when the expansion is carried out smoothly in an orbital environment. In contrast to the deployment simulation results in a grounded environment, the expansion in orbit takes 1.5 s for the whole deployment process, and the mass

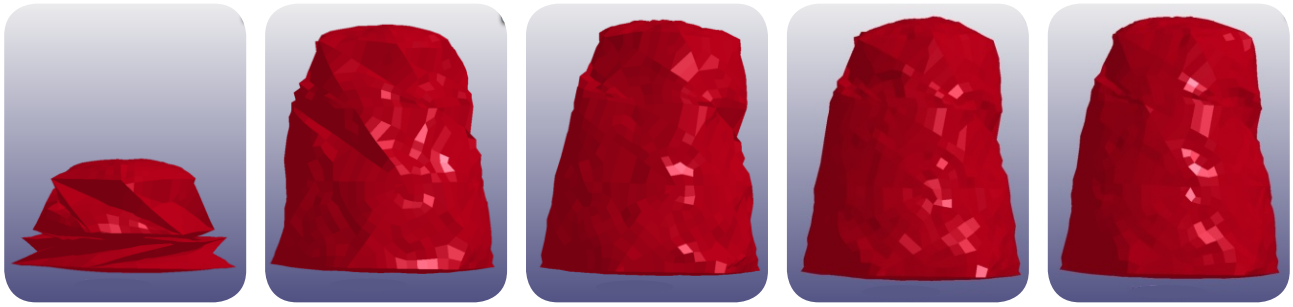

Figure 10. Deployment configurations of the inflatable capsule structure.

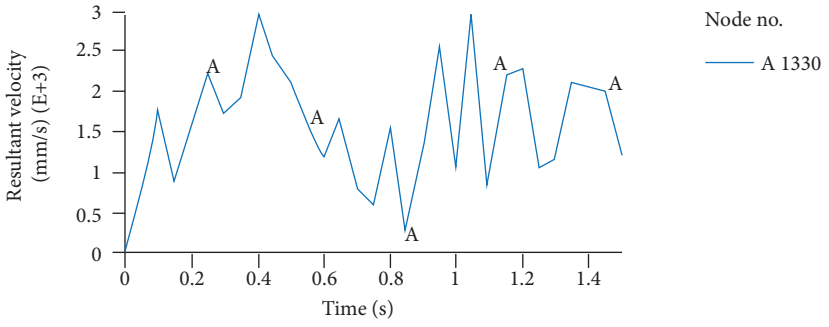

Figure 11. Velocity VZ-time curve of the top center node.

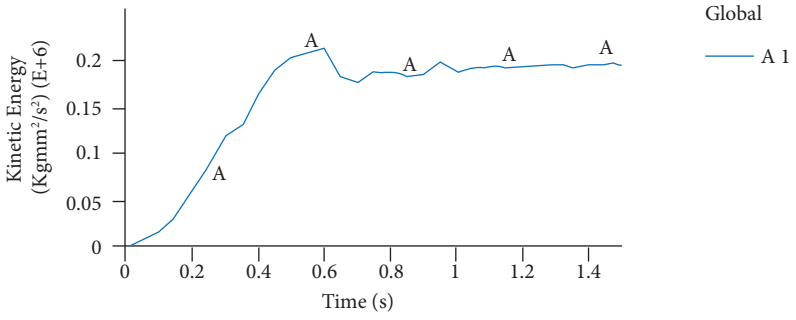

Figure 12. System kinetic energy-time curve.

of the inflatable gas is 7.5 g. The deployment time and inflation gas needed are approximately 1% of those needed in the ground environment experiment.

INFLUENCING MECHANISM OF RESIDUAL GAS

IMPACT ANALYSIS OF RESIDUAL GAS

In the process of packing the inflatable capsule structures, a residual gas inevitably remains in the chamber. Thus, it is necessary to analyze the effects of this residual gas on the folding, launch and final expansion of the inflatable capsule structures.

In the analysis, it was assumed that there is no gas in the chamber of the structures at initiation. When the structures are released, the gas (the quantity is equal to residual gas, such as 0.05 g) enters the structure in a very short amount of time (such as 0.01 s). The mass flow rate of the inflation gas is designed to be 5 g/s within 0.01 s, and then no inflation occurs after that. The deployment dynamics of the structures in this load case are simulated, and the final configuration of the inflatable capsule structures under the effect of the residual gas are shown in Fig. 13.

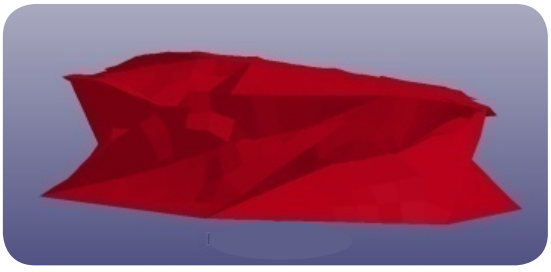

Figure 13. Final configuration of capsule structures.

To evaluate the deployment process under the effect of residual gases, the z displacement of the highest node in the top surface is analyzed. The z displacement of the central node in the top surface is shown in Fig. 14. The kinetic energy of the whole system is shown in Fig. 15. The analysis results show that the z coordinate of the highest node can reach 0.5 m under the effects of residual gases. Then, the z coordinate of the highest node returns to 0.3 m and maintains a dynamic balance state. With the effect of residual gases, it is difficult to pack an inflatable capsule structure into a small volume, requiring the launch space to be very large.

The influence of the residual gases on the subsequent expansion process is investigated. When the dynamic balance state is reached in 5 s, the inflation process is started again. The mass flow rate of the inflation gas is designed to be 1 g/s and the inflation time starts from 5 s to 12 s. The final configuration of the inflatable capsule structures under the effects of residual gases is shown in Fig. 16.

From the results, it can be seen that the inflatable capsule structure cannot be deployed smoothly. The main reason for this phenomenon is that the structure is deployed partly under the effect of residual gases before 5 s, which results in the upper and

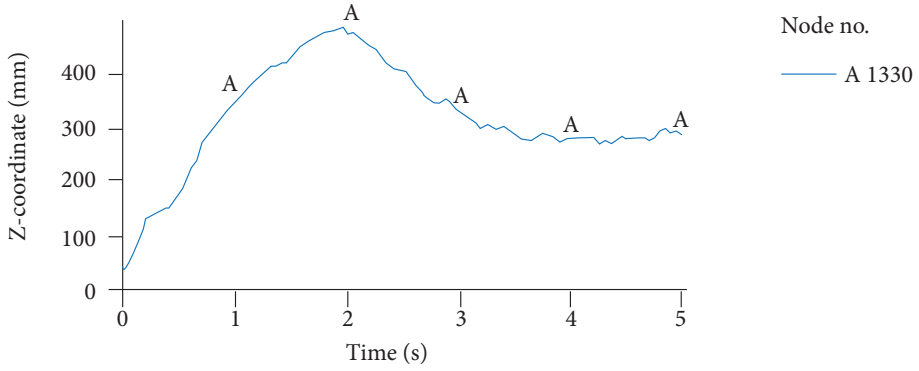

Figure 14. Z displacement-time curve of the top center node.

lower layers of thin film being glued together. Then, the extrusion pressure between the two layers of the thin film cease to be very large, which leads to fold creases that cannot be successfully opened under the subsequent inflation pressure.

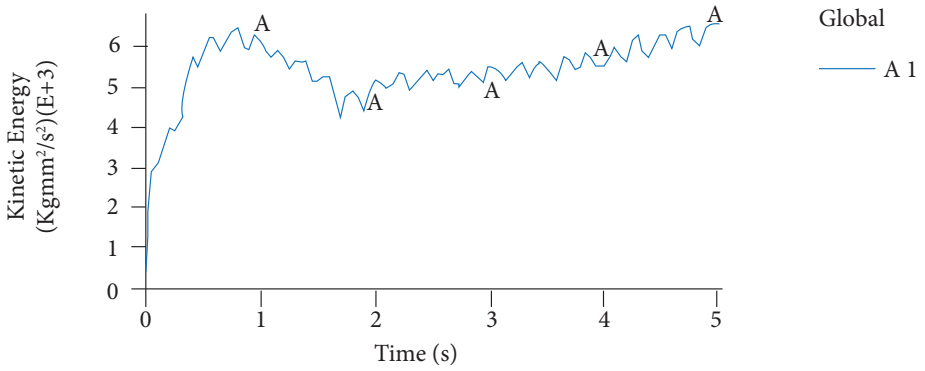

Figure 15. System kinetic energy - time curve.

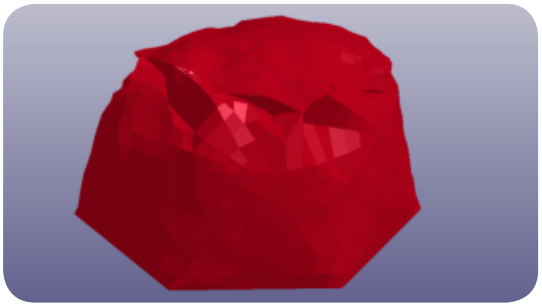

Figure 16. Final configuration of capsule structures.

METHODS TO ELIMINATE THE EFFECTS OF RESIDUAL GASES

To eliminate the adverse effects of the residual gases on the subsequent dynamic characteristics, theories and methods are needed. Two methods are presented that address this problem through the design of the inflation process.

Rapid inflation method

After the packaging devices of the inflatable capsule structure are released, the inflation gas is immediately fed into the chamber. Then, the structure is expanded using the original residual gas and the inflation gas that follows. The inflation process is assumed to start 1 s after the packing devices are opened. The mass flow rate of the inflation gas is designed to be 1 g/s, and the inflation time runs from 1 s to 8 s. The final configuration from the dynamic analysis is shown in Fig. 17. The membrane in the structure is not glued together, and the whole capsule structure can be expanded smoothly.

Preinflate method

As mentioned above, the mass of residual gas in the structural chamber is assumed to be 0.05 g. When using the pre-inflate method, 0.15 g of gas is added before the packaging devices of the inflatable capsule structure are released. The total mass of the internal gas at this point is 0.2 g. Then, by opening the packaging device, the inflatable capsule structure is deployed under the action of the gas until 5 s, when the dynamic balance state is reached. From the configuration of the structure, it can be seen that the membrane is still glued together. Then, the capsule structure is inflated again at a mass flow rate of 1 g/s and the period of deployment is 5-12 s. The final configuration of the inflatable capsule structure after the whole process is shown in Fig. 18. Using the pre-inflate method, the amount of residual gas can be artificially increased. From the simulation results, it is seen that the whole expansion process can be performed smoothly, and the adverse effects of residual gases can be overcome.

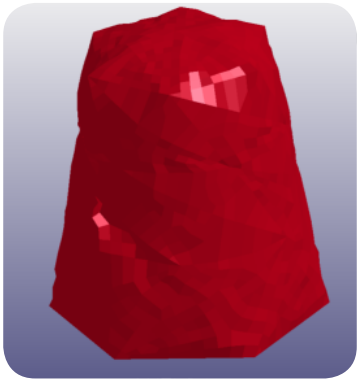

Figure 17. Deployed configuration of the rapid inflation method.

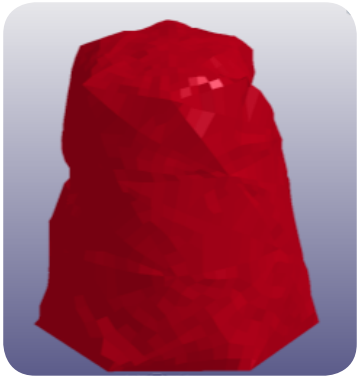

Figure 18. Deployed configuration from preinflate methods.

CONCLUSIONS

The six-fold-line folding pattern and deployment dynamic analysis model of an inflatable capsule structure were investigated in this paper. Especially, the influence of residual gases was considered in the deployment dynamic analysis model. The relation formulas of the fold angles were derived in detail, and the fact that the folding patterns meet the folding requirement of the spatial surface was proven. The folded state of the structure was obtained using parametric modeling, and a numerical simulation model of deployment dynamics was established. Based on the ANSYS/LS-DYNA software, a numerical analysis of the orbital deployment dynamics of the inflatable capsule structure was completed. The results show that there is no great collision or physical interference when the expansion is carried out smoothly. The feasibility of the folding pattern and the deployment dynamic analysis model were verified. The influence of residual gases to deployment process was investigated. In terms of the design of the inflation process, the rapid inflation method and pre-inflate method were presented to overcome the adverse effects of residual gases. The numerical analysis results verified the feasibilities of these methods.

When the inflatable capsule structure is folded by most of the folding pattern, the residual stresses inevitably appear in the membrane material, as does the strain energy stored in the folded configuration. In the future, the adverse effects of residual stresses from the folding process should be studied.

ACKNOWLEDGMENTS

This work was supported by the National Natural Science Foundation of China (Grant No. 11402229), the Zhejiang Province Natural Science Foundation (Grant No. LQ14A020003), and Quzhou science and technology plan project (No. 2016y006).

AUTHOR'S CONTRIBUTION

Conceptualization, Hong Y and Yao W; Methodology, Hong Y, Yao W and Xu Y; Investigation, Hong Y, Yao W and Xu Y; Writing – Original Draft, Hong Y, Yao W and Fang T; Writing – Review and Editing – Hong Y, Yao W, Xu Y and Fang T.

REFERENCES

Bouzidi R, Buytet S, Le van A (2013) A numerical and experimental study of the quasi-static deployment of membrane tubes. International Journal of Solids and Structures 50(5):651-661. doi: 10.1016/j.ijsolstr.2012.10.027

Clem AL, Smith SW, Main JA (2000) A pressurized deployment model for inflatable space structures. Presented at: 41st Structures, Structural Dynamics, and Materials Conference and Exhibit; Atlanta, USA. doi: 10.2514/6.2000-1808

Haug E, Protard JB, Milcent G, Herren A, Brunner O (1991) The numerical simulation of the inflation process of space rigidized antenna structures. In: ESA, Spacecraft Structures and Mechanical Testing 2:861-869.

Hinkle J, Lin JKH, Watson J (2009) Deployment testing of an expandable lunar habitat. Presented at: AIAA Space 2009 Conference and Exhibition; Pasadena, USA. doi: 10.2514/6.2009-6447

Lichodziejewski L, Kelley C, Tutt B, Jurewicz D, Brown G, Gilles B, Barber D, Dillman R, Player C (2012) Design and testing of the inflatable aero-shell for the IRVE-3 flight experiment. Presented at: 53rd AIAA Structures, Structural Dynamics and Materials Conference; Honolulu, USA. doi: 10.2514/6.2012-1515

Schenk M, Viquerat AD, Seffen KA, Guest SD (2014) Review of inflatable booms for deployable space structures: packing and rigidization. Journal of Spacecraft and Rockets 51(3):762-778. doi: 10.2514/1.A32598

Sosa EM, Wong CS, Barbero EJ, Thompson GJ (2016) Finite element simulation of deployment of large-scale confined inflatable structures. Thin Walled Structures 104:152-167. doi: 10.1016/j.tws.2016.02.019

Wang JT, Johnson AR (2003) Deployment simulation methods for ultra-lightweight inflatable structures. (ALR-TR-2973). NASA Technical Report.

Wei JZ, Tan HF, Wang WZ, Cao X (2015) Deployable dynamic analysis and on-orbit experiment for inflatable gravity-gradient boom. Advances in Space Research 55(2):639-646. 10.1016/j.asr.2014.10.024

Welch AL, Smith SW, Main JA (2003) Experimental results regarding two-dimensional deployment of inflatable beams. Presented at: 44th Structures, Structural Dynamis and Materials Conference; Norfolk, USA. doi: 10.2514/6.2003-1976

Xu Y, Guan FL, Chen JJ, Zheng Y (2012) Structural Design and Static Analysis of a Double-ring Deployable Truss for Mesh Antennas. Acta Astronautica 81(2):545-554. doi: 10.1016/j.actaastro.2012.09.004

Xu Y, Zheng Y, Guan FL, Huang H, Xu X (2015) Parametric model method and deployment simulation of inflatable antenna structures. Journal of Aerospace Technology and Management 7(2):219-230. doi: 10.5028/jatm.v7i2.395

Xu Y, Zheng Y, Kuang S, Zhou S (2016) Conceptual design of flexible thermal protect structure for deployable lunar habitats. Journal of Deep Space Exploration 3(2):168-174. doi: 10.15982/j.issn.2095-7777.2016.02.012